Journal of King Saud University – Engineering Sciences xxx (xxxx) xxx

Contents lists available at ScienceDirect

Journal of King Saud University – Engineering Sciences

journal homepage: www.sciencedirect.com

Original article

Evaluating the effects of recycled concrete aggregate size and concentration on properties of high-strength sustainable concrete

Md. Habibur Rahman Sobuz [a,*], Shuvo Dip Datta [a], Abu Sayed Mohammad Akid [a,b], Vivian W.Y. Tam [c], Shoaib Islam [a], Md. Jewel Rana [a], Farhad Aslani [d], Çağlar Yalçınkaya [e], Norsuzailina Mohamed Sutan [f]

[a] Department of Building Engineering and Construction Management, Khulna University of Engineering and Technology, Khulna 9203, Bangladesh
[b] Civil Engineering, Arkansas State University, Jonesboro, AR 72467, United States
[c] School of Built Environment, Western Sydney University, Australia
[d] School of Civil, Environmental and Mining Engineering, The University of Western Australia, Australia
[e] Department of Civil Engineering, Faculty of Engineering Dokuz Eylül University, İzmir Turkey
[f] Department of Civil Engineering Universiti Malaysia Sarawak, Kota Samarahan Sarawak 94300, Malaysia

ARTICLE INFO

Article history:
Received 29 July 2021
Accepted 25 April 2022
Available online xxxx

Keywords:
Recycled concrete aggregate
High strength concrete
Recycled aggregate concrete
Fresh properties
Mechanical properties
Sustainability

ABSTRACT

This paper studies the fresh and mechanical properties of high-strength concrete (HSC) by incorporating recycled concrete aggregates (RCA) of varying sizes and concentrations. The recycled aggregate concrete (RAC) was prepared by partially replacing RCA with natural coarse aggregate (NCA) at 0%, 15%, 30%, and 45%, with aggregate sizes ranging from 5 to 12 and 12–20-mm. Fresh concrete properties, such as slump, Kelly ball, compacting factor, K-slump, and fresh density, were tested to determine the influence of RCA size and concentration. In addition, the mechanical properties were studied through the execution of compressive, split-tensile, and stress-strain tests. The test results revealed that increasing the RCA concentration declines the fresh and hardened properties of HSC. In the fresh concrete experimentation, the 12–20 mm aggregate size RAC mixes exhibited greater workability than the 5–12 mm aggregate mixes. On the contrary, 5–12 mm aggregate mixes RAC had higher compressive and split-tensile strength and a higher modulus of elasticity than 12–20 mm aggregate mixes concrete. When it comes to sustainability, the study found that the smaller size range of RAC produces inferior embodied CO_2 (eCO_2) and provides a cost-effective and sustainable solution for the construction industry.

1. Introduction

Over the last decades, the construction community has faced several challenges, including a scarcity of natural resources and excessive energy consumption that directly impacts environmental pollution. These challenges include using natural resources and energy, the generation of greenhouse gases (CO_2), and the growth of building and demolition waste (Datta et al., 2022; Vo et al., 2021). Recycling the demolition waste is the most promising option for reducing the building industry's adverse environmental effects in the construction sector. This attention is increasingly growing since it was projected that the world has to reckon with the problems of disposing of 3 billion tons of demolished concrete waste annually until 2012 (Akhtar et al., 2018). In recent years, Zhang et al. (2020) reported that the global accumulative carbonation of concrete waste might produce roughly 3.0 Bt CO_2 between 2018 and 2035. As a result, using recycled concrete aggregate (RCA) made from waste concrete in engineering construction can

* Corresponding author.
E-mail addresses: habib@becm.kuet.ac.bd (Md. Habibur Rahman Sobuz), shuvodipkuet@gmail.com (S.D. Datta), asm.akid@becm.kuet.ac.bd (A.S.M. Akid), V.Tam@westernsydney.edu.au (V.W.Y. Tam), jewelrana@becm.kuet.ac.bd (M.J. Rana), farhad.aslani@uwa.edu.au (F. Aslani), caglar.yalcinkaya@deu.edu.tr (Ç. Yalçınkaya), msnorsuzailina@unimas.my (N.M. Sutan).
Peer review under responsibility of King Saud University.

Production and hosting by Elsevier

https://doi.org/10.1016/j.jksues.2022.04.004
1018-3639/

Please cite this article as: Md. Habibur Rahman Sobuz, Shuvo Dip Datta, Abu Sayed Mohammad Akid et al., Evaluating the effects of recycled concrete aggregate size and concentration on properties of high-strength sustainable concrete, Journal of King Saud University – Engineering Sciences, https://doi.org/10.1016/j.jksues.2022.04.004

help protect the environment while increasing the residual value of waste concrete. In addition, these RCAs have gained widespread acceptance from the construction research community as alternative building structure materials in recent decades. Several types of RCA research have been carried out for many years and are now being incorporated into new construction projects. The foremost challenges in producing recycled aggregate concrete (RAC) are its poor mechanical and unpredictable fresh properties (Huang et al., 2017). Consequently, the amount of recycled aggregate that can substitute normal coarse aggregate (NCA) in concrete has been limited due to these constraints. When recycled aggregate is used in the manufacture of high-strength concrete (HSC), the properties of the concrete can be less deficient than in normal concrete, which is an enticement for the construction industry (Gao et al., 2020).

Among the numerous properties of RAC, one of the most critical is its workability, which has a significant effect on its hardened properties (Kurda et al., 2017). It has been discovered that several investigations have been carried out on the limited characteristics of fresh RAC (Ait Mohamed Amer et al., 2016; Kurda et al., 2017). However, little effort was made in the experimental investigation to produce highly workable concrete with a variety of recycled aggregate gradations. Therefore, the undefined workability of fresh state concrete can be vulnerable to concrete placement, transport, compaction, finishing, and implementation time. According to Gao et al. (2020), the addition of RCA can alter the fresh characteristics of concrete due to its surface roughness, porosity, higher absorption nature, and greater angularity. As the concentration of RCA in the mix increases, the degree of workability decreases; however, using more superplasticizer (SP) increases may prevent slump declination (Matias et al., 2013). In contrast, Revilla-Cuesta et al. (2021) proposed that the water content in the concrete mix be adjusted to achieve the same workability of HSC as having RCA in the mix. The fresh density of RAC is significantly lower than that of normal concrete as pore spaces reduce RCA particles' specific gravity compared to NCA particles (Ismail & Ramli, 2013). Besides, the water absorption of RCA is higher than that of NCA, which could affect the workability behaviour (Thomas et al., 2018).

Ajdukiewicz and Alina (2002) investigated the mechanical properties of high-performance concrete (HPC), and high-strength concrete (HSC) made with RCA. They discovered that the compressive strength increased by approximately 10% when RCA was incorporated into the mixes. However, Xu et al. (2017) found that RAC strength was lower than normal strength concrete, resulting in micro-cracks in the old cement matrix that adhered to the periphery of RCA concrete specimens. Moreover, the compressive strength of RAC could be 10–25% lower than that of natural aggregate concrete (Bai et al., 2020). According to Sobuz et al. (2022), using RCA led to a decrement in the compressive strength of the concrete mix. Kou et al. (2012) concluded that substituting 20%, 50%, and 100% RCA reduced the split-tensile strength of concrete by 6.8%, 12.56%, and 21.6%, respectively, when compared to corresponding normal strength concrete. Similar results were obtained for mixes in which the splitting tensile strength declined due to the porosity of the RAC mixes (Mohammed Ali et al., 2020; Silva et al., 2015). Moreover, ACI (2002) building code correlated the modulus of elasticity (MOE) to the compressive strength of concrete and reported that the peak stress occurred at a peak strain of 0.002. Additionally, Thomas et al. (2018) observed that when RCA is completely replaced with NCA concrete, the MOE of the RAC decreases by approximately 34% due to the weaker initiation of the interfacial transition zone (ITZ).

The proportion of Portland cement and the aggregate type significantly affected the embodied CO_2 (eCO_2) discharges of concrete. Hanif et al. (2017) estimated that one ton of Portland cement emits around 931 kg of CO_2. Azúa et al. (2019) reported that substituting NCA for RCA reduced the costs and eCO_2 emissions associated with the construction of prefabricated concrete components. However, Bostanci et al. (2018) optimized the multi-criteria assessment to examine the environmental and economic benefits of RCA. Therefore, till now, no investigations have been carried out to observe the influence of different aggregate sizes with varying coarse aggregate (CA) concentrations on the sustainability of RAC.

2. Research significance

Previously, extensive research was conducted on recycled aggregates for producing normal strength concrete, self-compacting concrete, high-performance concrete, and ultra-high-performance concrete (Abed et al., 2020; Etxeberria, 2020; Gao et al., 2020; Mohammed Ali et al., 2020). However, previous studies have not attempted large-scale experimentation to quantify the fresh and mechanical properties of HSC in conjunction with the different size and concentration effects of RCA as a substitution for NCA in concrete mixtures. In this study, the authors attempted to incorporate the aggregates with a unique size range of 5–12- and 12–20-mm with 15%, 30%, and 45% concentrations of RCA mixes in NCA to produce moderate strength sustainable RAC. The slump, Kelly ball, compacting factor, K-slump, and fresh density tests were conducted to assess the fresh properties of RAC, while the compressive, split-tensile, and stress-strain responses were carried out to determine the mechanical properties. Moreover, the percentage replaced by RCA mixes was compared to plain HSC mixes. The statistical regression analysis was used to quantify the concrete properties with different codes of practice. Sustainability performance assessment represents social, environmental, and economic evaluations of the study's designated mixes that have yet to be investigated.

3. Experimental program

3.1. Materials

Ordinary Portland cement (OPC) of type I was used in this investigation which complies with ASTM C150 (ASTM, 2019). Silica fume, an amorphous polymorph of SiO_2, was employed to replace OPC for all concrete mixes. The chemical constituents of OPC and silica fume are presented in Table 1. The grading curve of fine aggregate, RCA and NCA are shown in Fig. 1. RCA particles were accumulated from the demolished waste of new academic buildings at Khulna University of Engineering and Technology, Khulna – 9203, Bangladesh. Because of the size limitation of the jaw crusher machine, the hand hammer was employed to reduce the size of the original concrete between 50 and 70 mm. With a maximum size of 25 mm, the jaw crusher was used to smash the original concrete to a greater extent. Furthermore, RCA was mechanically sieved and graded into aggregate sizes of 5–12 mm, and 12–20 mm and attained a fineness modulus close to NA. The specific gravity of aggregate was employed following ASTM C29/C29M (ASTM, 2017b), whereas the absorption of aggregate was obtained using ASTM C127-15 (International, 2015). The natural washed river Sylhet sand was employed as fine aggregate. Table 2 depicts the physical properties of CA, fine aggregate and RCA. The high-range water reducer, referred to as superplasticizer (SP), was incorporated in the manufacture of HSC. The fresh potable tap water was used in the concrete mixes, and the pH was 7.35.

3.2. Mix proportions and concrete mixing

Details of the concrete mix and proportions are presented in Table 3. The mix design was conducted by the following (ACI,

Table 1
Chemical properties of OPC cement and silica fume.

Constituents	Weight, %								
	SiO_2	Al_2O_3	Fe_2O_3	CaO	MgO	Na_2O	K_2O	SO_2	Loss of ignition
OPC	21.52	4.58	3.38	66.02	1.26	1.205	2.76	0.45	1.235
Silica fume	85	1.13	1.45	0.8	0.8	1.2	1.2	–	<5

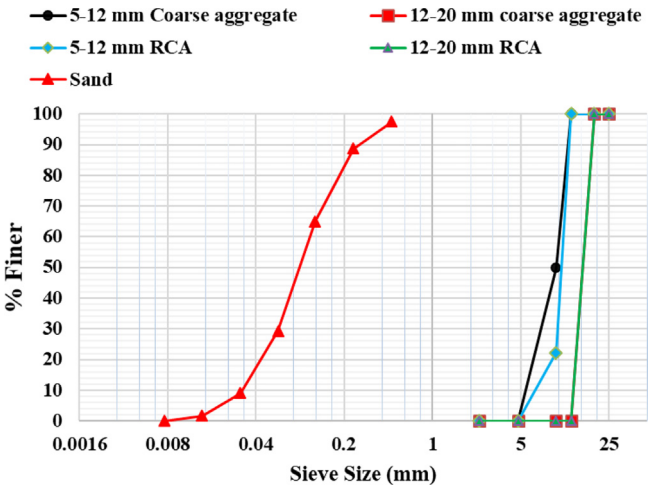

Fig. 1. Particle size distribution of aggregates.

1992). The concrete mixes were designated according to the varying concentration of RCA replacement rate at 0%, 15%, 30%, and 45% in the NCA, incorporating two different size ranges of the aggregate of 5–12 mm and 12–20 mm. Eight concrete mixes have been divided into two primary groups regarding both aggregate size ranges and referred to as "group – A" and "group – B", as shown in Table 3. The concrete's elemental mix composition comprises a 1:1.54:2.40 ratio of ordinary Portland cement, fine aggregate, and coarse aggregate. The water to binder ratio of control mixes was set as 0.33, considering the moisture content of aggregates. Moreover, the amount of water was compensated in the RAC mixes as the concentration of air-dried RCA was enhanced because RCA had a more significant water absorption capacity. The effective W/B ratio and effective water content were reported in Table 3 for all the mixes. Besides, silica fume was used as a 10% substitution of OPC. The control mix is identical to the traditional HSC mix, which contains 5–12 mm and 12–20 mm aggregate size ranges of NCA, and these mixes are designated as HSC5-0 (control mix-1) and HSC12-0 (control mix-2), respectively. The letter "HSC" stands for high-strength concrete, and the suffixes 5 and 12 represent aggregate size ranges with first numeric values. The final number represents the percentage of RCA replacement. In addition, the rest of the mixes are designated according to the varying concentration of 15%, 30% and 45% RCA replacement in the concrete, such as RCA5-15, RCA5-30, and RCA5-45 for 5–12 mm size range of aggregate; whereas, the corresponding RCA replacement of 12–20 mm size range of aggregate concrete mixes referred as RCA12-15, RCA12-30 and RCA12-45. The mixing procedure of all designated concrete mixes was performed according to ASTM C685 (ASTM, 2017a).

3.3. Specimen preparation, curing, and testing

The concrete was poured into 100×200 mm cylindrical moulds for all tests in this investigation. After that, the cylindrical specimens were cured in water for 7, 28, and 56 days at room temperature, 27 ± 2 °C, until the testing day. The fresh concrete slump test was determined by following ASTM C143 (ASTM, 2012). Besides, the slump value of concrete is affected by both plastic viscosity and yield stress. Hu et al. (1996) established a slump test quantification through the finite element model and provided an equation for yield stress by slump and density as presented in equation (1).

$$\tau_0 = \frac{\rho}{270} \times (300 - s) \quad (1)$$

Here, τ_0 = yield stress (Pa), s = slump value (mm), and ρ = density (kg/m^3).

The Kelly ball test of fresh concrete was determined based on ASTM C360-92 (ASTM, 1992). Compacting factor test of the freshly concrete mixes was tested complying with BS 1881 (BS, 1993). Besides, the K-Slump test can provide the workability variations and degree of compaction of fresh concrete complying with the standard ASTM (ASTM, 2009). Furthermore, the fresh concrete density was obtained following BS EN 12350B. Standard (2010). For the mechanical test of concrete, 168 cylindrical specimens were prepared in this investigation. Three specimens were tested for compressive, splitting tensile strength at 7, 28, and 56 days and stress-strain behaviour analysis of concrete at 28 days, respectively. The compressive strength test of the concrete specimens was performed following ASTM C39 (ASTM, 2018). Additionally, concrete cylindrical specimens were instrumented with four Linear Variable Displacement Transducers (LVDTs) at four corners of the platen to determine the stress-strain response. The mean value of the four $LVDT_S$ was calculated to get the final axial contraction. The split-tensile strength of concrete was tested according to the standard ASTM C496 (ASTM, 2017c).

Table 2
Physical characteristics of aggregate.

Characteristics	Sand	NCA		RCA	
		5–12 mm	12–20 mm	5–12 mm	12–20 mm
Specific gravity, G_S	2.34	2.64	2.72	2.52	2.58
Apparent specific gravity, Gsa	2.44	2.71	2.80	2.65	2.74
Water Absorption, %	1.82	1.04	1.08	5.89	5.05
Void ratio, e	40.51	46.44	47.24	51.55	49.03
Loose bulk density (kg/m^3)	1392	1414	1435	1221	1315
Compacted bulk density (kg/m^3)	1563	1583	1606	1337	1389

Table 3
Mix proportion of the concrete mixes (kg/m^3).

Group	Mix ID	Cement	Silica Fume	Sand	NCA	RCA	Effective Water	SP, %	Effective W/B
A	HSC5-0	500	50	772	1172	–	181	1.30	0.33
	RCA5-15	500	50	772	997	176	185	1.30	0.34
	RCA5-30	500	50	772	820	352	191	1.30	0.35
	RCA5-45	500	50	772	645	527	195	1.30	0.35
B	HSC12-0	500	50	772	1172	–	181	1.30	0.33
	RCA12-15	500	50	772	997	176	185	1.30	0.34
	RCA12-30	500	50	772	820	352	191	1.30	0.35
	RCA12-45	500	50	772	645	527	195	1.30	0.35

4. Results and discussions

4.1. Rheological state properties of RAC

4.1.1. Slump test

Fig. 2 represents the graphical illustration of the slump and yield stress of the varying concentration of RCA replacement in the concrete mixes. The test results indicated that the slump value followed a declining fashion when the concentration of RCA increased in the concrete mixture; however, the yield stress of fresh concrete demonstrated an increasing fashion for both sizes of aggregate range in the concrete mixtures. Besides, the greater aggregate size of 12–20 mm produced a higher slump than the 5–12 mm size of aggregate as the increased absorption rate of smaller aggregate particles leads to lesser slump recognition. More specifically, RCA's irregular shape and rough texture can cause grain-locking and resistance to mobility in concrete and mortar. Conversely, an average of 5.67% dropping in the slump is observed in RAC with respect to the HSC12-0 mix, whereas it is about 6.4% for RAC compared to HSC5-0. This decline in slump measurement is due to the incorporation of RCA in the concrete mixes that satisfied the test observation made by the researchers (Ait Mohamed Amer et al., 2016; Sun et al., 2020). Several researchers (Ajdukiewicz and Alina, 2002; Kou et al., 2012) also reported that water should be increased for RCA to uphold the similar workability of normal strength concrete. In addition, the harshness of the concrete mix rises attributed to RCA particles' rough texture, which reduces the workability at a higher RCA concentration of the concrete mixes. Further examining the test results from Fig. 2, the roughness of recycled aggregates enhanced during aggregate processing (throughout crushing) tends to reduce the flow properties,

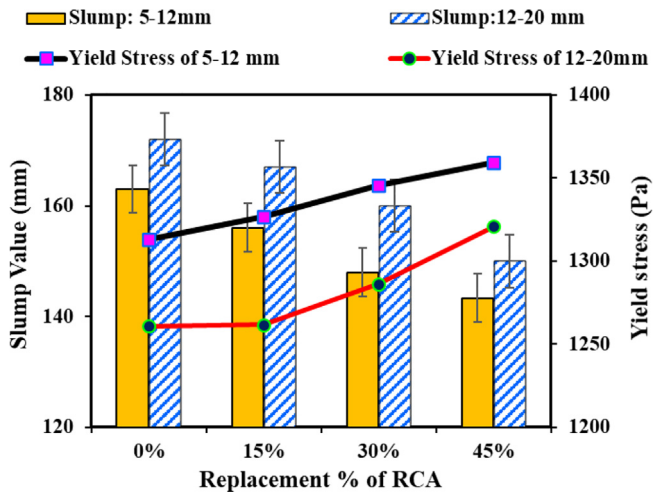

Fig. 2. Slump and yield stress for different replacements of RCA.

raising the yield stress of freshly mixed concrete. It is worth noting that 5–12 mm CA concrete displayed higher yield stress than the 12–20 mm aggregate concrete due to the flowability of smaller aggregate sizes in the mixes.

4.1.2. Compacting factor test

It can be noticed that the compacting factor value shows a decreasing trend with increasing the RCA concentration for both sizes range of RAC mixes, as illustrated in Fig. 3(a). For HSC5-0 and HSC12-0 concrete mixes, the compacting factor is found inferior in the HSC5-0 mix due to the grain-locking behavior of aggregate. The mixtures of RCA5-15, RCA5-30, and RCA5-45 have exhibited a reduction in compacting factor of about 0.79%, 1.80%, and 1.93% compared to the control samples (HSC5-0), respectively; while, RCA12-15, RCA12-30, and RCA12-45 demonstrated the reduction values of 0.60%, 1.03%, and 2.25% than the HSC12-0, respectively. The decrease in compacting factor with the RCA concentration replacement is due to recycled aggregates properties, which absorbed some of the mixing water and prevented the cement paste from flowing. Furthermore, for the high workability of fresh concrete, the compacting factor range should be 0.92–0.95 with the corresponding slump value of 100–175 mm, which satisfied the consistent finding with an experimental investigation conducted by Zeyad et al. (2018). Fig. 3(b) indicates a strong correlation between the compacting factor ($\mathbf{C_f}$) and the slump of concrete mixes ($\boldsymbol{s}$) for both aggregate sizes range concrete mixes. The minor variation in compacting factor among the aggregate size ranges may be attributed to the decreasing voids in the RCA concrete mixes for both aggregate size ranges.

4.1.3. Kelly ball penetration test

Fig. 3(a) shows that Kelly ball penetration value reduces steadily with the constant increase of RCA addition in RAC mixtures. The ball penetration value of RAC decreases around 3.3% on average than the respective control concrete of group – A; whereas it was obtained on average of 4.3% drops of the ball penetration value compared to the control concrete, which made with 12–20 mm aggregate size range. The water absorption properties and greater surface area of RCA are responsible for declining the concrete mixes' penetration value. Hence, it can be suggested to use presoaked RCA (Etxeberria, 2020) or higher quantities of SP (Matias et al., 2013) to lessen such a reduction of concrete workability. Conversely, concrete mixes in group – A exhibit lesser ball penetration values than the group – B mixes due to the filling of more voids, accumulation of maximum spaces with smaller aggregate, and interlocking behavior of aggregates. The slump value is obtained around 1.8 times with respect to the Kelly ball penetration value that could be used to predict the slump value through the Kelly ball penetration test. The action is similar to the investigation of Akid et al. (2021). Furthermore, Fig. 3(b) indicates a good linear correlation between the ball penetration value ($\boldsymbol{b_p}$) and the slump ($\boldsymbol{s}$) of both sizes ranges of aggregate concrete mixes. The

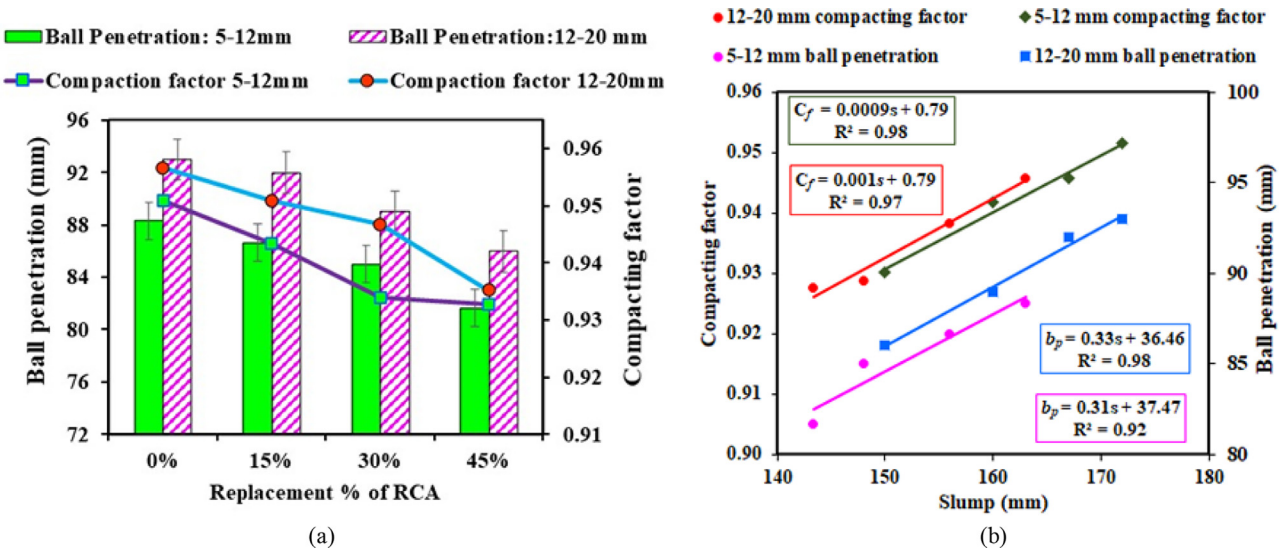

Fig. 3. (a) Kelly ball penetration and compacting factor for different replacement of RCA; (b) Correlation between compacting factor, slump and ball penetration.

5–12 mm aggregate size range mixtures trend line indicates that the aggregates with a high content of smaller coarse particles can have a lower dispersion due to increased antiparticle collisions nature.

4.1.4. K-slump Penetration test

K-slump test penetration values of RCA and control mixes of concrete are illustrated in Fig. 4. It should be noted that the K-slump penetration value shows a decreasing fashion with the addition of RCA for both sizes of aggregate, and an interestingly consistent decreasing trend in K-slump penetration is true for density value. It can be observed that the slump value obtained is around five times the K-slump value of RAC in this current investigation. K-slump illustrates a declining trend of the value around 10%, 19%, and 33% for RCA5-15, RCA5-30, and RCA5-45 mixes compared to HSC5-0, respectively; whereas, RCA12-15, RCA12-30, and RCA12-45 mixes exhibited 3%, 26%, and 38% decreasing of the value compared to HSC12-0 respectively. In addition, the decreasing reason for the K-slump penetration is similar to the slump test investigation (Ait Mohamed Amer et al., 2016; Kurda et al., 2017). The loss of cement matrix into the surface pores of RCA can also reduce the workability of the concrete. However, the rough texture

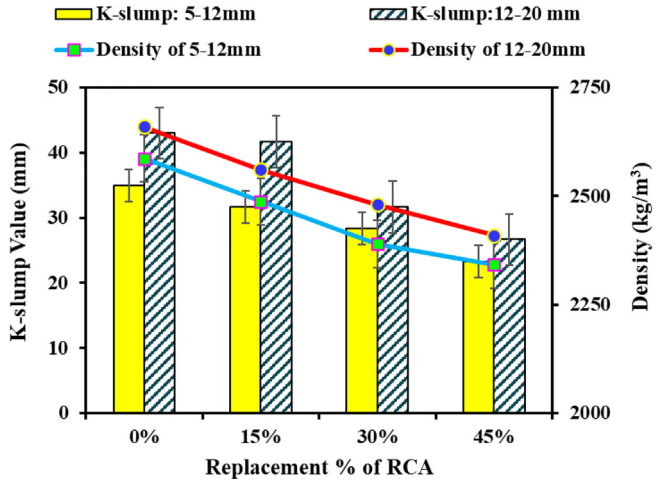

Fig. 4. K-slump value and density for different replacements of RCA.

of the angular RCA leads to the decreasing nature of the K-slump penetration value of the concrete mixes.

4.1.5. Density test

It is observed that the density of fresh concrete mixes reduces with the RCA concentration substitution increases in the RAC mixtures, as depicted in Fig. 4. In general, aggregate density, cement amount, water, and air content govern concrete density (Çakır, 2014). As per the current experimental investigation, 12–20 mm aggregate concrete mix indicates higher fresh density than the 5–12 mm aggregate concrete mix. On the other hand, fresh density shows a decrease of the value of about 3.9%, 7.6%, and 9.4% for RCA5-15, RCA5-30, and RCA5-45 mixes compared to the HSC5-0 mix, respectively; while, RCA12-15, RCA12-30, and RCA12-45 mixes demonstrate a decrease of the value approximately 3.7%, 6.7%, and 9.4% than the HSC12-0 mix, respectively. As expected, the mixes' density decreases with the incorporation of RCA particles as it has less density than the NCA. Furthermore, the angularity of the RCA can reduce compacting capacity, resulting in a lower fresh density of RAC. According to Ismail and Ramli (2013), RCA's specific gravity is subordinate to the NCA particles. Therefore, an increase in the concentration of RCA has a substantial influence on the reduction of concrete density.

4.2. Mechanical characteristics of RAC

4.2.1. Compressive strength

Varying statistical tools analyze the compressive strength test outcomes through mean strength, standard deviation, coefficient of variation (COV), standard error, and the 95% confidence interval at lower and upper ranges. It is noticed from the statistical analysis that the compressive strength varied from 24.07 MPa to 53.86 MPa at all curing age concrete specimens. It is noteworthy that RAC with varying RCA concentration attained an average of 69.38% and 102.68% of the 28-days compressive strength at 7- and 56-days curing period, respectively, for the group – A specimens; whereas it was achieved an average of 66.65% and 103.2% at same curing conditions for the group – B specimens. The standard deviation of the group – A concrete specimen ranges from 0.11 to 1.78 with the COV of 0.3% to 5.1%, and the standard error is varied from 0.064 to 0.462. Group – B concrete specimens exhibit a standard deviation of 0.14 to 1.97 with a range of COV of 0.32% to 5.7%, and the standard error varies the extent of 0.065 to 0.442. The

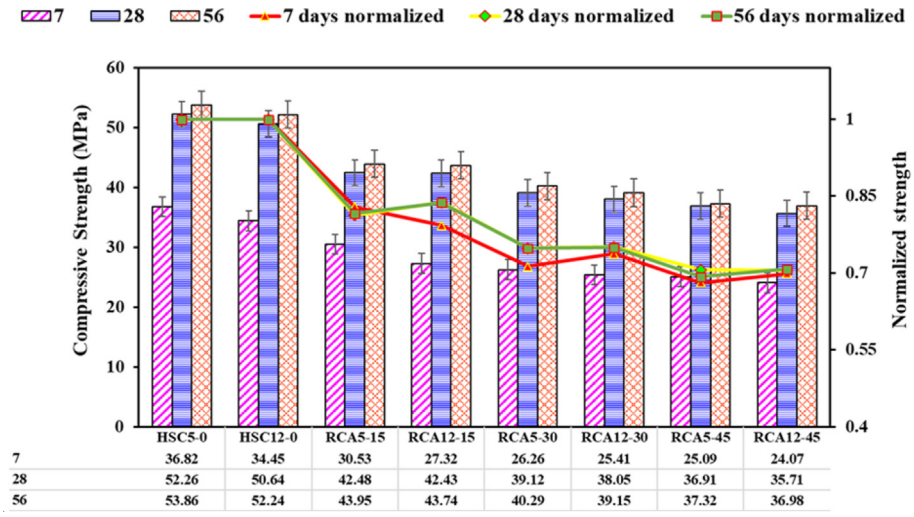

Fig. 5. Compressive strength and normalized strength of the concrete mixes.

compressive strength has the lowest value of 24.07 MPa at seven days specimen with a 95% confidence interval of 23.2 MPa to 24.94 MPa. In contrast, the compressive strength of 56 days specimens has the highest value of 53.86 MPa with a 95% confidence interval of 53.41 MPa to 54.31 MPa.

Fig. 5 showed that the compressive strength of group-A specimens was increased value by 3.1%, 0.48%, 2.91%, and 0.92% on average for the RCA replacement of 0, 15%, 30%, and 45%, respectively at 56 days as compared to the corresponding RAC specimens of group – B. In addition, the 7- and 28-days compressive strength also showed a similar kind of growth due to having a smaller aggregate size of 5–12 mm. Alternatively, the control specimen of HSC5-0 exhibited a 6.9%, 3.2% and 3.1% increase in compressive strength compared to the control specimen of HSC12-0 at 7, 28, and 56-days, respectively. It is noticed from this current investigation that the concrete specimens with smaller CA of the group – A have maximum effects in increasing the compressive strength at all curing ages. This smaller aggregate size concrete specimen increases the strength due to the interlocking behavior of aggregate, blocking more void spaces and more homogenous internal structure of the specimen. As a result, the identical replacement with the smaller size aggregate provides better compressive strength, which is quite similar to the investigation by Verma and Ashish (2017).

Fig. 5 also displays the normalized strength according to both control samples for 7, 28, and 56 curing ages for different concentrations of RCA mixtures. It is worth mentioning from Fig. 5 that the concrete specimen of RCA12-15 has attained the compressive strength of approximately 79.3%, 83.8%, and 83.7% compared to the specimen HSC12-0 at 7, 28, and 56 days respectively, whereas the corresponding strength achieved about 82.9%, 81.3%, 81.6% than the concrete specimen HSC5-0. The rest of the mixes having 30% and 45% replacement of two different sizes of aggregate specimens show lower normalized strength than the 15% concentration replacement of RCA in the concrete sample for all curing days. The decline in compressive strength with the RCA concentration increment denotes that the RCA creates a large number of voids in the concrete mixtures. Moreover, the cohesion force between the RCA surface and cement is weaker than the cohesion force between the NCA and cement matrix, which reduces strength. The concrete mix bond strength is mainly developed at the mortar phase, aggregate phase, and also the interface of the cement matrix, and therefore, aggregates play a vital role in this regard (Thomas et al., 2018). In the case of RAC, the RCA particles in the ITZ are not up to the mark compared to normal concrete because of the existence of the parent concrete's mortar adhered to it (Thomas et al., 2018). González-Fonteboa and Martínez-Abella (2008) also concluded that the inherent micro-cracks in ITZ sort its lower strength and increase the stress concentration at the crack orders due to the spread of hairline cracks in the concrete. Hence, compressive strength is affected progressively when the substitution level of RCA increases.

4.2.1.1. Crack propagation and failure patterns. The failure patterns due to compression testing of cylindrical control concrete and RAC specimens with varying concentrations of RCA at a 28-days testing period are represented in Fig. 6. An inclined fracture wedge surface is formed after the peak stress attained in cylindrical specimens of HSC5-0 and HSC12-0, and peripherical concrete

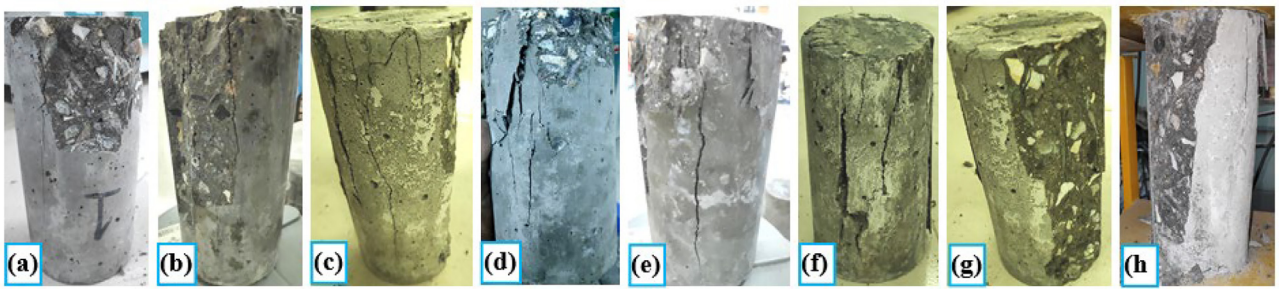

Fig. 6. Observed compressive strength failure patterns of the specimen at 28 days (a) HSC12-0; (b) HSC5-0; (c) RCA12-15; (d) RCA5-15; (e) RCA12-30; (f) RCA5-30; (g) RCA12-45; (h) RCA5-45.

starts spalling, leading to the so-called cone and shear failure mode as shown in Fig. 6(a and b). It can be noticed that the nature of the cracking in this wedge formation leads to a higher energy dissipation for the HSC5-0 and HSC12-0 cylindrical specimens. The specimen fracture pattern showed the confining effect of silica fume with the aggregate that tends to hold the materials together and countereffect the lateral tension. Therefore, the failure pattern of the concrete specimens showed ductile nature that ultimately provides time-dependent serviceability behavior of the member before final failure. The shear failure pattern was detected by the specimen RCA12-15 depicted in Fig. 6(c). Cone and shear failure propagation identified the RCA5-15 specimen, as illustrated in Fig. 6(d). Due to old adhered cement matrix RCA particles, the smaller aggregate spalls out from the mortar bonding. This behavior is consistent with the failure observation detected by Thomas et al. (2018) in their experimental study. The columnar failure pattern was observed for the RCA12-30 specimen; however, shear failure of the RCA5-30 cylindrical specimen occurred due to interlocking behaviour of smaller size ranges of aggregate as shown in Fig. 6(e and f). Furthermore, cone and shear failure wedge formation were observed more than the half-length of the specimens of RCA12-45 and RCA5-45, as depicted in Fig. 6(g and h).

4.2.2. Split-tensile strength

The experimental results of split-tensile strength of RCA mix with two different sizes of CA and varying concentrations are analyzed similarly to the compressive strength results with various statistical tools. It is noteworthy that RAC with varying RCA concentration was attained an average of 85.75% and 104.25% of the 28-days split-tensile strength at 7 and 56- days, respectively, for the group-A specimens; whereas the strength was achieved at an average of 87.05% and 105.23% at same curing conditions for group-B samples. According to the statistical observation, it can be noticed that the tensile strength extended from 3.06 MPa to 4.63 MPa for all concrete specimens with different curing ages. In this current investigation, the standard deviation varied from 0.017 to 0.122, with the range of COV of 0.4% to 2.7% and a standard error of 0.004 to 0.027. For 56 days, the highest mean tensile strength for the HSC5-0 concrete specimen was 4.63 MPa with a 95% confidence interval limit of 4.52 MPa to 4.74 MPa, whereas the HSC12-0 specimen showed 4.59 MPa with a 95% confidence interval of 4.48 MPa to 4.70 MPa.

Further assessing the test results, an increase in split-tensile strength was found due to adding a smaller aggregate than the larger aggregate size range in the concrete specimen, as depicted in Fig. 7. It can also be observed that the splitting strength of the specimen decreases as the RCA concentration increases in the mixes for both size ranges of aggregate. Besides, all the RCA concrete specimen compressive strength was achieved in the range of 83.7–91.4% of their 28-days strength at 7-days and 101.1–110.5% of their 28-day strength obtained at 56 days of curing ages. It is noticed that the highest concentration of RCA specimen decreases the splitting tensile strength up to 28.48% at 28-days for the larger size range of aggregate mix. The decreasing trend of the value is because of the weaker cohesion force between the RCA surfaces and cement matrix that enhances lower bond tendency in the concrete mix, and this conclusion is in line with the previous experimental findings (Ajdukiewicz and Alina, 2002; Silva et al., 2015). According to Thomas et al. (2018) experimental investigation, when the percentage of RCA is about 25%, the split-tensile strength of the concrete reduces by approximately 2–8%, which is quite similar to this study. However, González-Fonteboa and Martínez-Abella (2008) found that the inclusion of nano-particles of silica fume into the concrete mix can minimize the drop of splitting strength when replacing NCA with RCA.

It is clearly observed from Fig. 7 that a maximum tensile strength of about 3.43%, 1.1%, and 0.87% is found for the specimen HSC5-0 at 7, 28, and 56-day, respectively, compared to the specimen HSC12-0. This strength enhancement leads to the superior bonding characteristics of the smaller aggregates with the binder and the filling of void spaces by the smaller size aggregates. In contrast, the tensile strength reduces with RCA replacement percentage increment at all curing ages than in the control mixes, as presented in Fig. 7. The split-tensile strength reduces in a range of 3.2%-18.9% for the RAC specimen compared to the control sample HSC5-0, whereas the strength value decreases by 5.5%-28.5% with respect to the control sample HSC12-0. This behavior is attributed to the greater porosity of RAC that leads to a higher split-tensile strength reduction which satisfied the previous experimental investigation (Mohammed Ali et al., 2020; Silva et al., 2015).

4.2.2.1. Crack propagation and failure patterns. The splitting tensile testing failure patterns of cylindrical specimens with various concentrations of RCA replacement in NCA at 28-days testing are presented in Fig. 8. It can be noticed that the HSC5-0 and HSC12-0 failed in a brittle manner with a single smaller crack width at the specimen's mid-height under uniaxial loading, as shown in Fig. 8

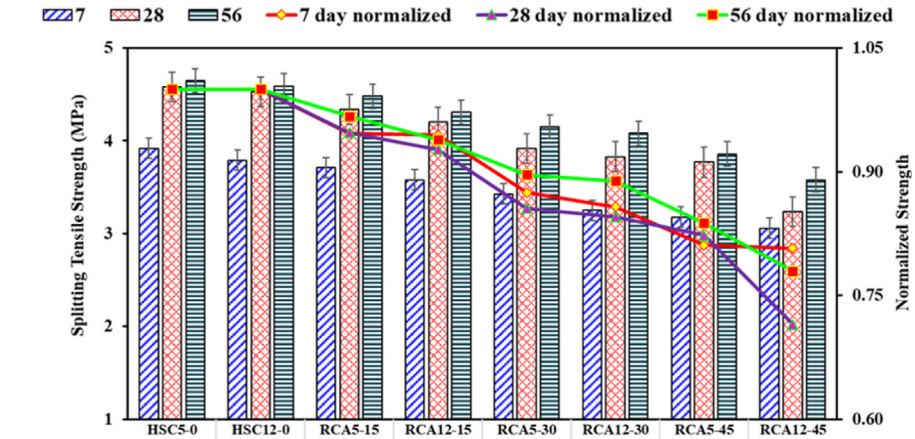

Fig. 7. Splitting tensile strength and normalized strength of the concrete mixes.

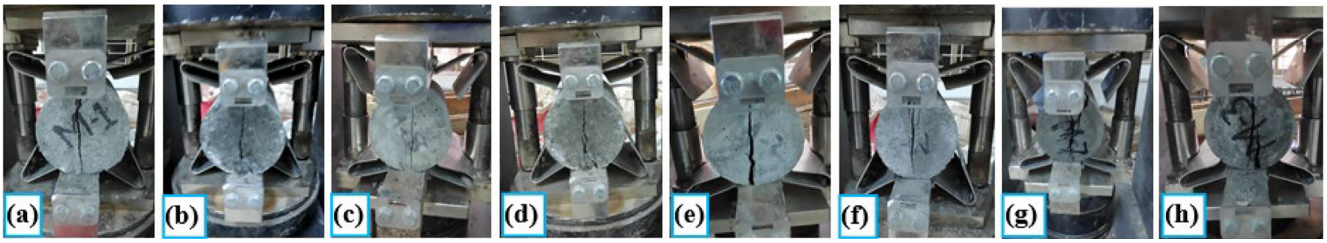

Fig. 8. Observed splitting failure patterns of the specimen at 28 days (a) HSC12-0; (b) HSC5-0; (c) RCA12-15; (d) RCA5-15; (e) RCA12-30; (f) RCA5-30; (g) RCA12-45; (h) RCA5-45.

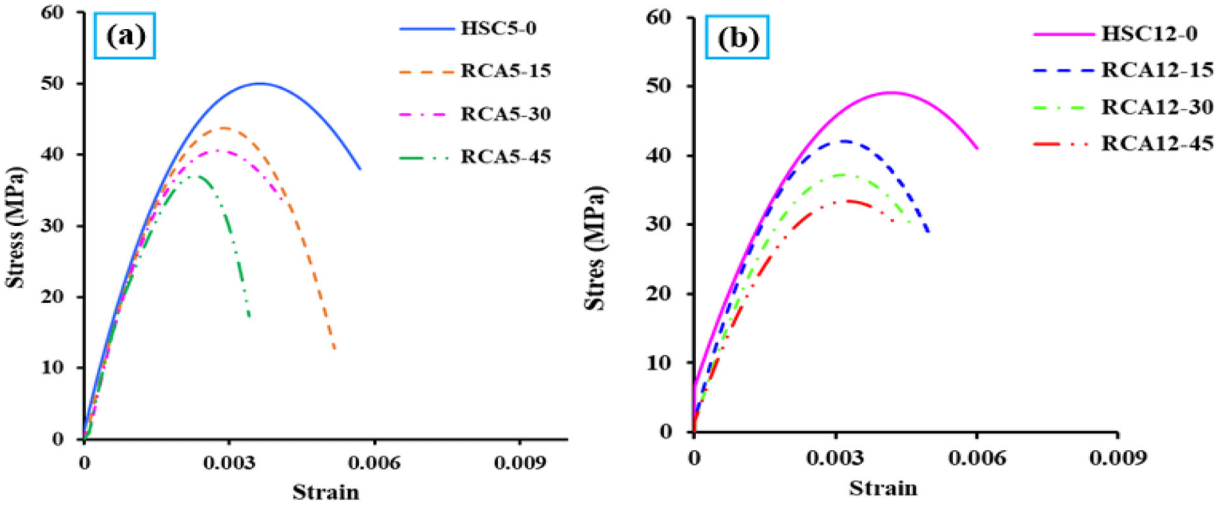

Fig. 9. Stress-strain diagram of RAC with size range of (a) 5–12 mm (b) 12–20 mm.

(a and b). It is worth noting that the crack pattern of concrete specimens was observed primary crack when they split out. It indicates that the smaller aggregate size with silica fume can control the crack of the HSC and prevent the specimens from falling apart. Further, examining failure nature, the brittle nature of primary crack was first initiated for RCA12-15, RCA5-15, RCA12-30, and RCA5-30 concrete specimens, and then it followed the secondary or multiple distributed cracking and a bit wider crack width along the diameter afterwards the whole length of the specimens as presented in Fig. 8(c and f). Besides, secondary or multiple cracking was developed along with the primary crack for RCA12-45 and RCA5-45, as shown in Fig. 8(g and h), which showed a more brittle nature than the previous cylindrical specimens. The higher concentration of RCA particles developed multiple distributed cracking at the softening stage of loading. As the concentration of RCA particles increases, the fracture path tracks the concrete's weakest zones, such as pore space, due to the inherent bond between RCA and cement mortar matrix.

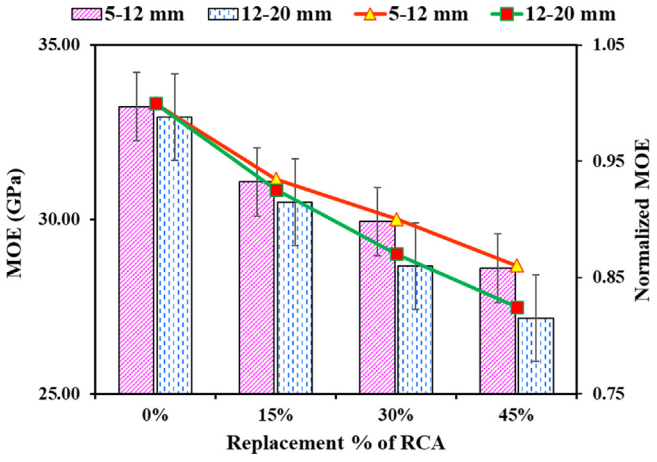

Fig. 10. MOE and normalized MOE with respect to control concrete mixes.

4.2.3. Stress-strain responses

The stress-strain responses of RAC specimens are presented in two different graphs in Fig. 9. It can be observed that the concrete with varying concentrations of 5–12 mm size range of RCA in Fig. 9 (a) showed relatively lower peak strain and residual strain compared to the size range of 12–20 mm RCA as referred to Fig. 9(b). The observation indicates that the larger aggregate size did not densify well enough due to the presence of more void space in the cement matrix and less homogeneity in the mix than the smaller aggregate size. Furthermore, in Fig. 9, for both size ranges of RCA, the ascending branch of all the curves exhibited a nearly linear slope until the peak stress. However, the slope of softening branch decreases as the recycled aggregate concentration decreases, demonstrating the greater overall energy absorption performance. The linear ascending branch slope phenomenon is more pronounced for 5–12 mm size aggregate concrete specimens, whereas the descending branch showed a higher contraction value for 12–20 mm size concrete mixture. It is also clearly seen that the varying concentration of the RAC specimen possessed a snap-back behavior or a bit more brittle properties than the control specimen for both sizes ranges of RCA. The behavior suggests that an increase in the size of CA upsurge the roughness of the aggregate surface. In

Table 4
Formulations of compressive strength and split tensile strength of concrete in different design codes.

Source	Relationship	Range, MPa
ACI 363R-92 (ACI, 1992)	$f_{sp} = 0.59f_c^{0.5}$	$21 \le f'_c \le 83$
ACI 318-08 (ACI, 2008)	$f_{sp} = 0.56f_c^{0.5}$	–
CEB-FIP (1990)	$f_{sp} = 0.3f_c^{2/3}$	$f'_c \le 83$
AS 3600(Standard, 2001)	$f_{sp} = 0.4f_c^{0.5}$	–
EHE (1998)	$f_{sp} = 0.21f_c^{2/3}$	–
GB 50,010 (GB, 2002)	$f_{sp} = 0.19f_c^{0.75}$	–
NBR 6118 (NBR, 2003)	$f_{sp} = 0.3f_c^{2/3}$	–
Current Study	$f_{sp} = 0.68f_c^{0.48}$	$f'_c \le 55$

Table 5
Formulations of compressive strength and modulus of elasticity of concrete in different design codes.

Source	Relationship	Range, MPa
ACI 363R-92 (ACI, 1992)	$E_c = 3{,}320(f'_c)^{0.5} + 6{,}900$	$21 \le f'_c \le 83$
CEB-FIP (1990)	* $E_c = 21{,}500\alpha_E(f'_c/10)^{1/3}$	$f'_c \le 80$
GB 50,010 (GB, 2002)	$E_c = \frac{10^5}{2.2+34.7/f'_c}$	–
Norges (Standard, 1992)	$E_c = 9500(f'_c)^{0.3}$	$25 \le f'_c \le 85$
Current Study	$E_c = 5136(f'_c)^{0.47}$	$f'_c \le 55$

* α_E = 1.2 for basalt, dense limestone aggregates; 1.0 for quarzitic aggregates; 0.9 for limestone aggregates; 0.7 for sandstone aggregates.

addition, void initiation in the concrete leads to an expansion in the stress concentration and transmission of cracks within the ITZ. Thus, the results turned into a brittle nature of the RAC compared to the control concrete. This finding is consistent with Nath et al. (2021), as they reported that the decline in the contraction of RAC leads to the addition of varying concentrations of recycled aggregate. The behaviour of the brittle nature of RAC could be improved by adding a small amount of steel fibre to the concrete mix, and further study is required to achieve the substantial ductility of the RAC. Afterwards, these properties could be incorporated into numerical modelling to quantify the structural behavior of the members.

The stress-strain relationships are affected by different parameters such as MOE, peak strain, corresponding stress at peak strain, type of concrete, measurement methods, and load speed. MOE has been determined from the linear ascending part of the stress-strain response of the curve, as depicted in Fig. 10. It can also observe from Fig. 10 that the peak strain of larger size aggregate RCA specimen increases because of the decreased elastic modulus of RAC, which indicates a larger deformation capacity of the concrete specimen. In comparison with the control concrete of group – B, RCA12-15, RCA12-30, RCA12-45 concrete specimens were shown about 7.42%, 12.94%, 17.52% decrease of MOE, respectively. In addition, the same percentage replacement of 5–12 mm aggregate size mixes demonstrates a lower normalized reduction in MOE with respect to the group – A control specimen than the group – B specimen. According to Thomas et al. (2018), an average 30% – 34% reduction in the MOE was perceived when 25% – 100 % of the NCA was substituted with RCA. In that case, the previous results showed less degradation than the current analysis because of silica fume. The presence of this ultra-fine silica powder provides a better mortar matrix stage in mixes, which produces higher stiffness among the concrete mix and increases the specimens' MOE value.

4.3. Relationship of the mechanical properties

Table 4 depicts the formulations of compressive and split-tensile strength of the concrete according to the various code of standard (ACI, 1992; ACI, 2008; CEB-FIP, 1990; EHE, 1998; GB, 2002; NBR, 2003; Standard, 2001). The split-tensile (f'_{spt}) and the compressive strength (f'_c) of the test results show a good correlation with a good coefficient of regression for the different code of standards, as illustrated in Fig. 11(a). It is observed that the tensile strength is about 7–8% of the compressive strength of concrete. It can also be noticed that the tensile strength of RCA mixes increases substantially with the increase of compressive strength value, and these enhancements are nearly constant throughout the analysis. It is clearly observed that the equation of CEB-FIP (1990) and NBR (2003) are close enough predictions to the current investigation; however, AS3600 and EHE are shown to have the furthest estimation from the confidence band (CB) and prediction band (PB). However, long parts of the prediction zone were covered by the ACI 363R-92 code, and it exhibits very well estimation compared to other codes of standards. The high splitting tensile strength creates the upward prediction line from the others standard due to the incorporation of smaller aggregate in the concrete mixes. Therefore, the aggregate interlocking effect enhances the splitting tensile strength properties of the concrete mixes.

Fig. 11(b) represents the relationship between the compressive strength (f'_c) and the modulus of elasticity (E_c) of concrete with the comparison of various codes of standard. The concrete compressive

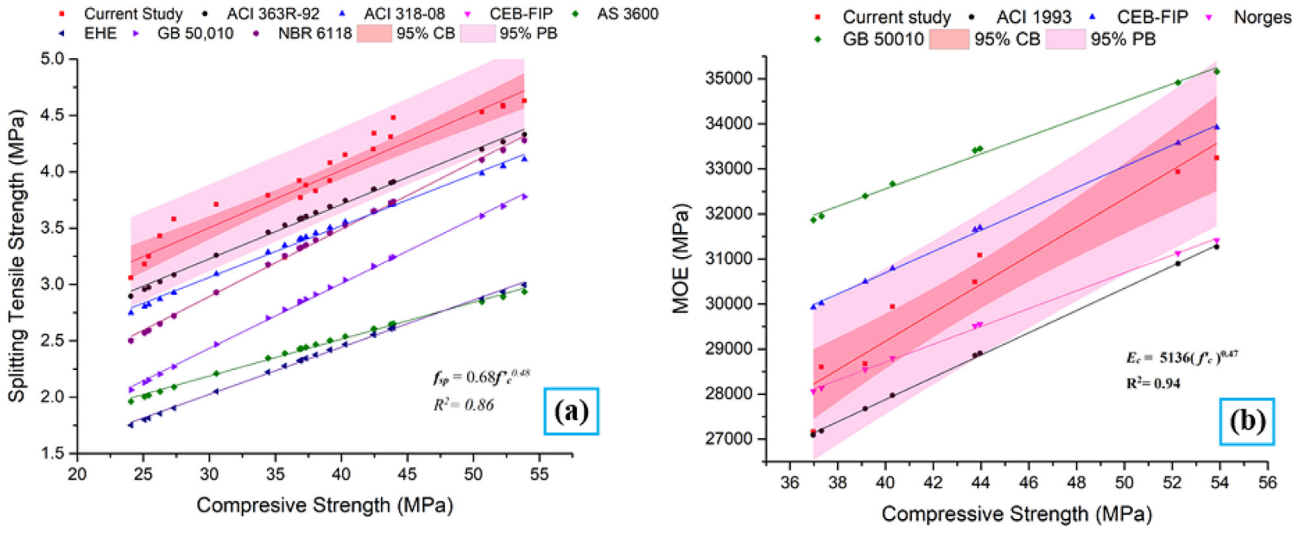

Fig. 11. Relationship between (a) Splitting tensile strength and compressive strength of concrete; (b) MOE and compressive strength of concrete.

Table 6
Material embodied energy and cost at the production and transportation stages

Materials	Material embodied Energy (MJ/kg)	eCO_2 emission kg CO_2/kg	eCO_2 emission kg CO_2/kg	Production cost (tk/kg)	Transportation cost (tk/kg)
	Production		Transportation		
NCA	0.083[(1)]	0.005[(1)]	0.021*	5	0.26
Cement	5.5[(1)]	0.95[(1)]	0.021*	9	0.34
Water	0.0009[(2)]	0.00155[(2)]	—	0.088	-
Admixture	0.0058[(1)]	0.0022[(1)]	0.086*	100	5
Fine aggregate	0.08[(4)]	0.0048[(4)]	0.16*	2.17	0.22
Silica Fume	0.036[(3)]	0.0028[(3)]	0.086*	34.75	5
RCA	0.066[(1)]	0.003[(1)]	—	-	0.67

Where, (1) Hammond et al. (2011)(2) Bostanci (2020) (3) Mineral Product Association (2009) (4) (Datta et al., 2022); Murthy and Iyer (2014)
* Transportation eCO2 emissions were estimated by taking the fact of travel distance from the pulling out to the production site in collaboration with the supplier company. The cost was assessed in BDT (1 USD = 84.53 Tk).

Table 7
Summary of eCO_2 emission concrete mixes.

Mix ID	Total CO_2 Emission	Production Emission	Transportation Emission	Production %	Transportation %	Cost (tk/m^3)
HSC5-0	647.38	485	162.38	74.92	25.08	15434
HSC12-0	648.55	485	163.55	74.78	25.22	15434
RCA5-15	643.36	484.66	158.70	75.33	24.67	14631
RCA12-15	644.53	484.66	159.87	75.20	24.80	14631
RCA5-30	639.28	484.30	154.98	75.76	24.24	13818
RCA12-30	640.45	484.30	156.15	75.62	24.38	13818
RCA5-45	635.26	483.95	151.31	76.18	23.82	13015
RCA12-45	636.43	483.95	152.48	76.04	23.96	13015

strength and MOE formulations in different design codes are presented in Table 5. The expression of this current study is quite similar to the CEB-FIP (1990), as their values cover the 95% confidence band in the analysis. On the other hand, ACI (ACI, 1992) and Norges N. Standard (1992) estimation also cover the 95% prediction interval with a bit of deviation to MOE of the current investigation. However, the MOE value decreases with the percentage replacement of RCA due to the inferior strength gaining of the aggregate–mortar ITZs. In addition, the MOE of concrete can be affected by the aggregate's elastic modulus (Li et al., 2019). Therefore, ACI (ACI, 1992) estimation range slightly deviates from the 95% prediction band of MOE from this current study at a higher strength value of concrete with two different size ranges of aggregate.

4.4. Sustainability assessment

Material embodied energy and cost at production and transportation stages are presented in Table 6 to evaluate the sustainability criteria of the mixes. Total eCO2 emissions of various concrete mixes for transportation and production are represented in Table 7, obtained from Table 6. The eCO_2 emissions of the HSC12-0 and HSC5-0 mixes are about 648.55 kg CO_2/m^3 (278 kg CO_2/t) and 647.38 kg CO_2/m^3 (277 kg CO_2/t), respectively. The amount of eCO_2 emission decreases with the increment of partial replacement of RCA, as represented in Table 7. The group – B control mix exhibits a maximum eCO_2 emission rate than all other mixes. In addition, HSC5-0, RCA5-15, RCA5-30 and RCA5-45 mixes were reduced about 0.18%, 0.8%, 1.43% and 2.05% of eCO_2 emissions respectively; whereas, RCA12-15, RCA12-30 and RCA12-45 mixes decreased approximately 0.62%, 1.25%, and 1.87% of eCO_2 emissions respectively from the baseline emission of HSC12-0. The processing, marketing, and transportation of natural aggregates consume a lot of energy stored as embodied energy in the control concrete mixes. The eCO_2 emission of the mixes decreases with partial replacement as RCA particles can reduce energy-consuming virgin materials. The eCO_2 emission also decreases when the transportation length of the aggregate particle is small at the higher replacement level. The mix with 5–12 mm RCA shows better performance than 12–20 mm in terms of eCO_2 emission for transportation as any transporting vehicle can hold more small aggregate particles than large ones. RCA5-45 shows the best performance to reduce the eCO_2 emissions among other concrete mixes because of the highest replacement of virgin materials, around 45%, and optimized transportation length. Though RCA12-45 can reduce the highest amount of eCO_2 emission, it negatively reduces concrete strength significantly, as per the current investigation. Hence, this study suggests the RCA5-30 mix as an optimum solution because of has low eCO_2 emission and optimum strength.

This study also conducted an economic analysis to get the cost of the individual mix due to production and transportation costs, as represented in Table 7. It is described in Table 7 that the cost per m^3 of concrete decreases with the increment of partial replacement of RCA. It can also be noticed that both sizes of aggregate concrete need the same amount of cost. The maximum cost was obtained at around 15,444 tk/m^3 for 0% replacement of the RCA concrete mix. RCA5-45 and RCA12-45 mixes represent the most cost-efficient concrete production rate at 13,015 tk/m^3 ensuring 15.67% cost savings compared with the control mix's cost. Although 45% replacement of RAC reduces the highest cost for the production of per m3 concrete, it also has a negative effect of decreasing concrete strength considerably, according to the current study. Like the eCO_2 assessment, this study suggests the RCA5-30 mix as an optimum solution because of having low cost and optimum strength.

5. Conclusions

In this paper, the size and concentration effect of RCA on the production of HSC has been studied. Eight concrete mixes with different RCA concentration levels with an interval of 15% were considered. The obtained experimental results of the rheological and mechanical properties are concluded as follows:

- All the mixes had a satisfactory slump result greater than 150 mm, which led to the high workability of concrete. Concrete mixtures of the 12–20 mm aggregate size range have a larger slump, compacting factor, ball penetration, and K-slump value than the 5–12 mm size range concrete. In addition, the high density and workability of mixes decrease with an increasing concentration of RCA replacement level.
- The decrease in the split-tensile strength of RAC with the increase of the RCA concentration is relatively smaller than compressive strength and MOE. The 5–12 mm coarse aggregate size enhances the strength and MOE of the mixes compared to the 12–20 mm aggregate size. In terms of sustainability assessment, the cost and eCO_2 emission decrease with RCA incorporation, leading to a low-cost and environment-friendly concrete production with better strength.
- Analytical prediction of different codes of practice gives a strong estimation with MOE but a conservative prediction with splitting tensile strength compared to the current study. In contrast, several codes of practice demonstrated a scatter estimation with the experimental data. This analytical prediction, which will abide by RAC properties and ultimately reduce the cost of testing, suggests the further alteration of the estimation, labour, and time.
- In terms of sustainability assessment, the cost and the overall assessment indicate that it is feasible to produce greater than 40 MPa concrete with 5–12 mm RCA up to 30% replacement, saving 1.43% emission of eCO_2 than the control concrete. This optimum replacement percentage of RCA is recommended to produce low-cost sustainable concrete in the construction industry.

Further work could be done to improve the HSC capacity. It is recommended that the inclusion of steel fiber could improve strength and post-peak ductility behaviours having a large scatter concentration of RCA with varying fiber types and fiber slenderness factor.

Declaration of Competing Interest

The authors declare that they have no known competing financial interests or personal relationships that could have appeared to influence the work reported in this paper.

Acknowledgements

The authors wish to thank the Structural and Material Engineering Laboratory technicians in the Department of Building Engineering and Construction Management at Khulna University of Engineering and Technology, Khulna – 9203, Bangladesh, for overall support in specimen preparation and fabrication and testing period. This research did not receive any specific grant from funding agencies in the public, commercial, or not-for-profit sectors.

References

Abed, M., Nemes, R., Tayeh, B.A., 2020. Properties of self-compacting high-strength concrete containing multiple use of recycled aggregate. Journal of King Saud University – Engineering Sciences 32 (2), 108–114. https://doi.org/10.1016/j.jksues.2018.12.002.

Aci, 1992. State-of-the-art report on high-strength concrete. American Concrete Institute, Farmington Hills, Michigan.

ACI. (2002). Building code requirements for reinforced concrete (ACI 318-02) and commentary (ACI 318R-02). In (pp. 443): American Concrete Institute;.

ACI. (2008). *Building code requirements for structural concrete (ACI 318-08) and commentary*.

Ait Mohamed Amer, A., Ezziane, K., Bougara, A., Adjoudj, M., 2016. Rheological and mechanical behavior of concrete made with pre-saturated and dried recycled concrete aggregates. Construction and Building Materials 123, 300–308.

Ajdukiewicz, A.K., Alina, 2002. Influence of recycled aggregates on mechanical properties of HS/HPC. Cement and Concrete Composites 24 (2), 269–279. https://doi.org/10.1016/S0958-9465(01)00012-9.

Akhtar, Ali Sarmah, K.A., 2018. Construction and demolition waste generation and properties of recycled aggregate concrete: A global perspective. Journal of Cleaner Production 186, 262–281. https://doi.org/10.1016/j.jclepro.2018.03.085.

Akid, A.S.M., Hossain, S., Munshi, M.I.U., Elahi, M.M.A., Sobuz, M.H.R., Tam, V.W.Y., Islam, M.S., 2021. Assessing the influence of fly ash and polypropylene fiber on fresh, mechanical and durability properties of concrete. Journal of King Saud University – Engineering Sciences. https://doi.org/10.1016/j.jksues.2021.06.005.

M.P. Association The Concrete Industry Sustainability Performance Report 2009 Retrieved from.

ASTM. (1992). Test Method for Ball Penetration in Freshly Mixed Hydraulic Cement Concrete. In *C360-92*. West Conshohocken, PA: ASTM International.

ASTM. (2009). Standard Test Method for Flow of Freshly Mixed Hydraulic Cement Concrete In *C1362-09*. West Conshohocken, PA: ASTM International.

ASTM. (2012). Standard Test Method for Slump of Hydraulic-Cement Concrete. In *C143/C143M-12*. West Conshohocken, PA,: ASTM International.

ASTM. (2017a). Standard Specification for Concrete Made by Volumetric Batching and Continuous Mixing. In (Vol. C685/C685M-17). West Conshohocken, PA: ASTM International.

ASTM. (2017b). Standard Test Method for Bulk Density ("Unit Weight") and Voids in Aggregate. In *C29/C29M*. West Conshohocken, PA: ASTM International.

ASTM. (2017c). Standard Test Method for Splitting Tensile Strength of Cylindrical Concrete Specimens. In *ASTM C496*. West Conshohocken, PA, 2017: ASTM International.

ASTM. (2018). Standard Test Method for Compressive Strength of Cylindrical Concrete Specimens. In *ASTM C39/C39M-18*. West Conshohocken, PA: ASTM International.

ASTM. (2019). Standard Specification for Portland Cement. In *ASTM C150/C150M-19a*. West Conshohocken, PA.

Azúa, G., González, M., Arroyo, P., Kurama, Y., 2019. Recycled coarse aggregates from precast plant and building demolitions: Environmental and economic modeling through stochastic simulations. Journal of Cleaner Production 210, 1425–1434. https://doi.org/10.1016/j.jclepro.2018.11.049.

Bai, G.Z., Liu, C., Liu, C., Biao., 2020. An evaluation of the recycled aggregate characteristics and the recycled aggregate concrete mechanical properties. Construction and Building Materials 240,. https://doi.org/10.1016/j.conbuildmat.2019.117978 117978.

Bostanci, S.C., 2020. Use of waste marble dust and recycled glass for sustainable concrete production. Journal of Cleaner Production 251,. https://doi.org/10.1016/j.jclepro.2019.119785 119785.

Bostanci, S.C., Limbachiya, M., Kew, H., 2018. Use of recycled aggregates for low carbon and cost effective concrete construction. Journal of Cleaner Production 189, 176–196. https://doi.org/10.1016/j.jclepro.2018.04.090.

BS, 1993. Method for determination of compacting factor. BS 1881: Part 103. British Standards Institution, London.

Çakır, Ö., 2014. Experimental analysis of properties of recycled coarse aggregate (RCA) concrete with mineral additives. Construction and Building Materials 68, 17–25. https://doi.org/10.1016/j.conbuildmat.2014.06.032.

CEB-FIP. (1990). CEB-FIP Model Code for concrete structures, Euro-International Committe for Concrete. *Bulletin*(213/214).

Datta, S.D., Rana, M.J., Assafi, M.N., Mim, N.J., Ahmed, S., 2022. Investigation on the generation of construction wastes in Bangladesh. International Journal of Construction Management 1–10. https://doi.org/10.1080/15623599.2022.2050977.

Ehe, 1998. Spanish code for structural concrete. In. Real Decreto, Madrid.

Etxeberria, M. (2020). 13 – The suitability of concrete using recycled aggregates (RAs) for high-performance concrete. In F. D. Pacheco-Torgal, Yining Colangelo, Francesco Tuladhar, Rabin Koutamanis, Alexander (Ed.), *Advances in Construction and Demolition Waste Recycling* (pp. 253-284): Woodhead Publishing.

Gao, C.H., Yan, L., Jin, L., Chen, R., Haoze., 2020. Mechanical properties of recycled aggregate concrete modified by nano-particles. Construction and Building Materials 241,. https://doi.org/10.1016/j.conbuildmat.2020.118030 118030.

GB. (2002). Chinese standard: code for design of concrete structures. In *50010*. Beijing(China): China building press.

González-Fonteboa, B., Martínez-Abella, F., 2008. Concretes with aggregates from demolition waste and silica fume. Materials and mechanical properties. Building and Environment 43 (4), 429–437.

Hammond, G., Jones, C., Lowrie, E.F., Tse, P., 2011. Embodied carbon. Inventory of carbon and energy version 2.

Hanif, A., Kim, Y., Lu, Z., Park, C., 2017. Early-age behavior of recycled aggregate concrete under steam curing regime. Journal of Cleaner Production 152, 103–114. https://doi.org/10.1016/j.jclepro.2017.03.107.

Hu, C., deLarrard, F., Sedran, T., Bonlag, C., Bose, F., Deflorenne., 1996. Validation of BTRHEOM, the new rheometer for soft-to-fluid concrete. Materials and Structures 29 (194), 620–631.

Huang, L., Chen, L., Yan, L., Kasal, B., Jiang, Y., Liu, C., 2017. Behavior of polyester FRP tube encased recycled aggregate concrete with recycled clay brick aggregate: Size and slenderness ratio effects. Construction and Building Materials 154, 123–136. https://doi.org/10.1016/j.conbuildmat.2017.07.197.

International, A. (2015). Standard Test Method for Relative Density (Specific Gravity) and Absorption of Coarse Aggregate. In *ASTM C127-15*. West Conshohocken, PA.

Ismail, S., Ramli, M., 2013. Engineering properties of treated recycled concrete aggregate (RCA) for structural applications. Construction and Building Materials 44, 464–476. https://doi.org/10.1016/j.conbuildmat.2013.03.014.

Kou, S.C., Poon,, &, S.,, C., 2012. Enhancing the durability properties of concrete prepared with coarse recycled aggregate. Construction and Building Materials 35, 69–76. https://doi.org/10.1016/j.conbuildmat.2012.02.032.

Kurda, R., de Brito, J., Silvestre, J.D., 2017. Influence of recycled aggregates and high contents of fly ash on concrete fresh properties. Cement and Concrete Composites 84, 198–213.

Li, Y., Li, Y., Wang, R., 2019. Quantitative evaluation of elastic modulus of concrete with nanoidentation and homogenization method. Construction and Building Materials 212, 295–303.

Matias, D., De Brito, J., Rosa, A., Pedro, D., 2013. Mechanical properties of concrete produced with recycled coarse aggregates–Influence of the use of superplasticizers. Construction and Building Materials 44, 101–109.

Mohammed Ali, A.A.Z., Ahmed, R.S., Waleed, T., 2020. Evaluation of high-strength concrete made with recycled aggregate under effect of well water. Case Studies in Construction Materials 12,. https://doi.org/10.1016/j.cscm.2020.e00338 e00338.

Murthy, A.R., Iyer, N.R., 2014. Assessment of Embodied Energy in the Production of Ultra High Performance Concrete (UHPC). International Journal of Students Research in Technology & Management 2 (3), 113–120.

Nath, A.D., Hoque, M.I., Datta, S.D., Shahriar, F., 2021. Various recycled steel fiber effect on mechanical properties of recycled aggregate concrete. International Journal of Building Pathology and Adaptation ahead-of-print(ahead-of-print). https://doi.org/10.1108/IJBPA-07-2021-0102.

Nbr, 2003. design of concrete structures, In 6118. Brazilian association of technical standards, Rio de Janeiro.

Revilla-Cuesta, V., Evangelista, L., de Brito, J., Ortega-López, V., Manso, J.M., 2021. Effect of the maturity of recycled aggregates on the mechanical properties and autogenous and drying shrinkage of high-performance concrete. Construction and Building Materials 299,. https://doi.org/10.1016/j.conbuildmat.2021.124001 124001.

Silva, R.V., de Brito, J., Dhir, R.K., 2015. Tensile strength behaviour of recycled aggregate concrete. Construction and Building Materials 83, 108–118. https://doi.org/10.1016/j.conbuildmat.2015.03.034.

Sobuz, M.H.R., Datta, S.D., Rahman, M., 2022. Evaluating the Properties of Demolished Aggregate Concrete with Non-destructive Assessment. Paper presented at the Advances in Civil Engineering, Singapore.

Standard, A., 2001. Concrete structures. *AS-3600*. Standards Australia International, Sydney.

Standard, B. (2010). Testing fresh concrete Part 6: Density. In. EN.

Standard, N. (1992). Concrete structures—Design rules. In *NS 3473*. Oslo.

Sun, C., Chen, Q., Xiao, J., Liu, W., 2020. Utilization of waste concrete recycling materials in self-compacting concrete. Resources, Conservation and Recycling 161,. https://doi.org/10.1016/j.resconrec.2020.104930 104930.

Thomas, J., Thaickavil, N.N., Wilson, P.M., 2018. Strength and durability of concrete containing recycled concrete aggregates. Journal of Building Engineering 19, 349–365. https://doi.org/10.1016/j.jobe.2018.05.007.

Verma, S.K., Ashish, D.K., 2017. Mechanical behavior of concrete comprising successively recycled concrete aggregates. Advances in concrete construction 5 (4), 303–311.

Vo, D.-H., Hwang, C.-L., Tran Thi, K.-D., Yehualaw, M.D., Liao, M.-C., Chao, Y.-F., 2021. HPC produced with CDW as a partial replacement for fine and coarse aggregates using the Densified Mixture Design Algorithm (DMDA) method: Mechanical properties and stability in development. Construction and Building Materials 270,. https://doi.org/10.1016/j.conbuildmat.2020.121441 121441.

Xu, J., Chen, Z., Xue, J., Chen, Y., Liu, Z., 2017. A review of experimental results of steel reinforced recycled aggregate concrete members and structures in China (2010–2016). Procedia engineering 210, 109–119.

Zeyad, A.M., Tayeh, B.A., Saba, A.M., Johari, M.A.M., 2018. Workability, Setting Time and Strength of High-Strength Concrete Containing High Volume of Palm Oil Fuel Ash. The Open Civil Engineering Journal 12 (1), 35–46.

Zhang, N.D., Miller, H., Tam, T.R., Liu, V.W.Y., Zuo, G., Jian., 2020. Mitigation of carbon dioxide by accelerated sequestration in concrete debris. Renewable and Sustainable Energy Reviews 117,. https://doi.org/10.1016/j.rser.2019.109495 109495.